A new surface forces apparatus for nanorheology

Frédéric Restagno[a)]
Laboratoire de Physique, École Normale Supérieure de Lyon, 46 allée d'Italie, 69364 Lyon cedex 07 and Département de Physique des Matériaux, Université Claude Bernard, Bat. Léon Brillouin, 43 boulevard du 11 Novembre 1918, 69622 Villeurbanne cedex, France

Jérôme Crassous[b)]
Laboratoire de Physique, École Normale Supérieure de Lyon, 46 allée d'Italie, 69364 Lyon cedex 07, France

Élisabeth Charlaix, Cécile Cottin-Bizonne, and Michel Monchanin
Departement de Physique des Matériaux, Université Claude Bernard, Bat. Léon Brillouin, 43 boulevard du 11 Novembre 1918, 69622 Villeurbanne cedex, France

(Received 11 October 2001; accepted for publication 4 March 2002)

We present an original surface forces apparatus which enables us to measure the interaction forces between any solid surfaces such as, e.g., metallic surfaces, opaque surfaces, or rough surfaces. The relative displacement of the surfaces is measured with a capacitive sensor. The forces are measured by a stiff and highly sensitive interferometric sensor. The measurements are performed in a dc to 100 Hz bandwidth. This feature allows us to study the mechanical response of a nanometric confined medium to rapid strain variations in the linear regime. An example of nanorheological measurement of dodecane confined in a nanometric gap is given at the end of this article. © *2002 American Institute of Physics.* [DOI: 10.1063/1.1476719]

I. INTRODUCTION

The mechanical properties of soft matter at nanometric scale are now currently investigated using surface forces apparatus (SFA). These apparatuses have been originally built to measure van der Waals forces.[1,2] These apparatuses were then further developed to allow measurements in liquids, with applications in different fields including interactions between charged or grafted surfaces, confinement induced phases transitions, mesomorph phases, rheology, and more recently biophysical problems. The surface forces apparatus measures the force between two macroscopic surfaces as a function of surfaces separation. For this, one surface is mounted on a spring, whose bending is measured at the same time as the separation between surfaces. The important characteristics of this kind of apparatus are the distance and force resolutions, the choice of solid surfaces, and the dynamics of the measurements. These characteristics vary greatly with the choice of sensors used for the force and the separation measurement.

The most common SFA is the so-called interferometric SFA.[1] In this technique, collimated white light is transmitted through the surfaces, which generally are atomically smooth mica. A thin metallic layer on the back side of each mica sheets acts as an optical mirror, producing sharp interference fringes of equal chromatic order (FECO) in the focal plane of an imaging spectrograph. Determination of FECO wavelengths allows the simultaneous determination of the surfaces separation, the refractive index of the intersticial medium, and the shape of the surfaces. A first limitation of this technique is the time needed for the analysis of the fringes pattern, which limits the temporal resolution to roughly 1 s. Moreover, the constraint that solid surfaces must be both transparent and optically smooth, limits the practical choice of surfaces to mica, glass, or silica.

The limitations of this system may be avoided by reporting the measurement on mechanical part rigidly fixed to surfaces. In such a geometry, contrary to the common interferometric SFA, the deflection of the force-measuring cantilever is directly measured. The two main advantages of such a design is the free choice of surfaces, and the possibility of using fast and accurate electronic or optic sensors. The main drawback of this geometry is the difficulty in determining the origin of the displacements.

The use of capacitive sensors has been proposed for such SFA sensors.[3–6] The main advantages of these sensors are: the price, the ability to measure very large displacements, and the temporal resolution of the measurements. A first limitation of these sensors, for SFA use, is the resolution. Indeed, important resolutions may be achieved with small gaps between the capacitor plates, but the plates positions are hard to control.[7,8] With gaps between the capacitor plates smaller than a few micrometers, capillary condensation in a vapor atmosphere can occur and make the experiment impossible. A second limitation of the capacitive sensors is the need of a calibration in order to obtain an absolute distance measurement. These drawbacks are absent in the very high resolution interferometric sensor proposed recently in some atomic force microscopy setup.[9,10] However, its dynamic range is limited to one optical wavelength.

The present article describes an original dynamic surface forces apparatus (DSFA) where these two kinds of sensors

a)Present address: Laboratoire des Fluides Organisés, Collège de France, 11 place Marcelin Berthelot, 75005 Paris, France.
b)Author to whom correspondence should be addressed; electronic mail: jerome.crassous@ens-lyon.fr

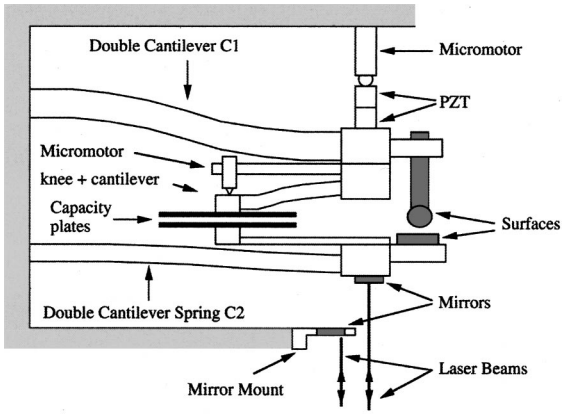

FIG. 1. Schematic drawing of the SFA.

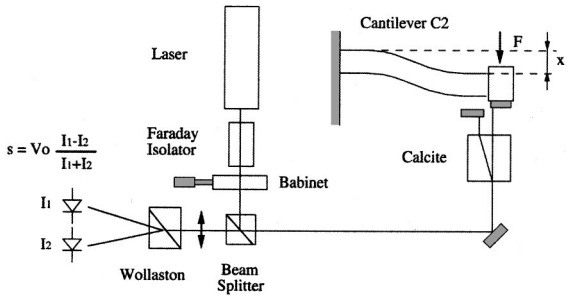

FIG. 2. Schematic drawing of the polarization interferometer used for the measurement of the cantilever bending.

are associated. In one hand, the force spring bending is measured with an interferometric sensor that offers a high resolution. On the other hand, the separation between the surfaces is measured with a capacitive sensor. This design does not need transparent surfaces since the relative displacement of the surface is not measured in the contact area. With this apparatus the use of almost any solid surface is now possible. The time response of the sensors authorizes dynamical studies up to 100 Hz. Since the distance between solid surfaces and the force spring bending deflection are independently measured, no assumption on the piezoelectric crystal linearity, which ensures surface displacement, is needed. In Sec. II we describe the mechanical parts of the apparatus and its sensors. In Sec. III we present the data acquisition system and we discuss the resolution of the apparatus. In Sec. IV, we propose a measurement of the hydrodynamic behavior of a confined dodecane nanometric liquid film as a test experiment.

II. APPARATUS

A. General description

A general diagram of the DSFA is shown in Fig. 1. This apparatus measures the statical and dynamical forces between two macroscopic surfaces (generally a plane and a sphere) as a function of their relative displacement. An important feature is to allow only a pure translational motion of the surfaces. For this, the two surfaces are firmly clamped on two double cantilevers C_1 and C_2. These cantilevers prevent any rotation of the surfaces. The relative motion of the surfaces is obtained with the help of a translation stage, which pushes the extremity of the cantilever C_1. This translation stage is composed of three elements. First, a 30 nm step micromotor[11] is used for a rough positioning of the surfaces at the beginning of the experiments. The initial distance between the surfaces is typically comprised between 1 and 3 μm. Second, fine displacements of the surfaces are performed by two piezoelectric actuators.[11] The first one, driven with a voltage ramp, allows a 5 μm continuous approach or recede of the surfaces. The second one is driven with a sinusoidal voltage to add a small sinusoidal motion (on the order of a fraction of nanometer) to the continuous motion.

The extremity of the second cantilever C_2 is free so that the deflection of C_2 measures the forces acting on it. A mirror is glued on it and is included in an interferometer detailed in the following section. The relative displacement of the surfaces is measured with a capacitive sensor which makes the measurements independent of the response of the two piezoelectric elements. For this purpose two 5-cm-diam duralumin plates are connected to the cantilevers extremities and form a plane capacitor. A ball and socket joint allows us to adjust the parallelism of the plates. The distance between the two capacitor's plates may be adjusted with another 30 nm step micromotor associated with a cantilever. We emphasize the fact that the capacitor plate mounted on C_2 is rigidly bound to the surface holder. The consequence is that during a cantilever deformation, the capacitor plate and the surface holder are translated on the same distance, whatever the cantilever deformation.

In addition, a small magnet is stuck on C_2 in front of a coil. This system allows us to apply a force on the cantilever and is used for the mechanical and electronic calibration. This system has been previously used by Stewart[4] and allows a displacement without any hysteresis. The frame of the DSFA is composed of 2-cm-thick duralumin plates. Each mechanical element is rigidly screwed to this structure and can be independently removed for cleaning.

The apparatus is covered with a simple 1-cm-thick plexiglass box which ensures a crude thermal isolation and sound vibrations isolation. The latter is put down on an antivibration table. The table is made up of a granite table top which is weighted down to roughly 1 ton with a dozen concrete blocks fixed under it. This is put on four coil springs. Finally, the table is on a stone slab lying down on the rock and disconnected from the building in order to minimize soil transmitted vibrations.

All the acquisitions during the experiments are performed in a separate room to prevent any vibration or thermal drift due to the operator.

B. Force sensor

The deflection of the force cantilever C_2 is measured with a differential interferometer based on the well known Nomarski principle.[7] It closely follows the setup of Schöenberger *et al.*[9] Its principle is shown in Fig. 2. The laser is a 1 mW polarized and stabilized He–Ne laser.[11] The laser beam passes through a Faraday isolator in order to protect the laser against back reflections. After the isolator, the beam's polar-

ization is close to 45° relative to the (*s*) and (*p*) beams in order to obtain the intensities of the two beams roughly equal: $I_p \approx I_s$. A Babinet compensator permits us to adjust the relative phase shift between these two polarization states. After passing a nonpolarizing beamsplitter and a mirror, the two beams arrive on a calcite crystal. The two emerging beams are orthogonally polarized and laterally separated by 1.2 mm. One of the beams is reflected by the mirror glued onto the cantilever and the other one onto the reference mirror. The parallelism of the two mirrors is ensured with a simple optical mount. After reflection and back return though the calcite plate, the two beams are recombined. The two components (*s*) and (*p*) of the electric field have a phase shift ϕ between them which is the sum of the phase shift $\Delta\phi = 4\pi x/\lambda$ due to the cantilever displacement and a phase shift ϕ_0 which takes into account shifts in the Babinet compensator and calcite plate. A Wollaston prism is used to produce interferences between these two polarization states. For a best contrast of interferences, the prism is diagonally oriented with respect to the two planes of polarization (*s*) and (*p*). The intensity I_1 and I_2 of the two beams is thus:

$$I_{1,2} = \frac{(I_s + I_p)}{2}[1 \pm m \cos(\phi_0 + \Delta\phi)],$$

where $m = 2\sqrt{I_p I_s}/(I_s + I_p)$ is the contrast. The two beams are focalized on two PIN silicon photodiodes[11] and the output current signals are amplified by operational amplifiers. With the aid of a voltage divisor,[11] we determine that

$$V = V_0 \frac{I_1 - I_2}{I_1 + I_2} = CV_0 \cos(\phi_0 + \Delta\phi) + V_{\text{off}}, \quad (1)$$

where $V_0 = 10$ V is a constant voltage, V_{off} is some offset voltage, and C is the overall contrast, typically $C \sim 0.9$, which takes into account small angular error in the position of birefringent elements, slight errors in the parallelism of mirrors, and differences in gains of photocurrent–voltage converters.

The visibility and offset are calibrated by imposing a large bending of a few λ to the cantilever with the help of the coil magnet system. The maximum and minimum values of V are thus measured, allowing a determination of both C and V_{off}. The sensibility $\Delta V/\Delta x = (CV_0 4\pi/\lambda)\sin(\phi_0 + \Delta\phi)$ is maximized by setting $\phi_0 = \pi/2[2\pi]$ with the help of the Babinet compensator. Indeed, for sufficiently small displacements ($x < \lambda/8$), the sensibility $\Delta V/\Delta x \approx (CV_0 4\pi/\lambda)$ is constant, and is typically $\Delta V/\Delta x \approx 0.2$ V/nm. For more important displacements, Eq. (1) is inverted in order to measure x. Photodiodes and electronic components have been chosen in order that their response times are negligible compared to the time scale of mechanical motions. This point has been checked by measuring the electronic response to a modulized light flux issued from a light emitting diode.

The practical resolution of this sensor is limited by the mechanical vibrations of our cantilever. Discussion of such vibrations and their effects on the resolution of the force sensor is reported in Sec. II. The resolution of this interferometer is measured when the two beams are sent on the same mirror. Figure 3 represents the equivalent displacement noise spectrum as a function of the frequency in this configuration. Above 700 Hz, the noise is close to both the expected electronic noise of the voltage divisor (5×10^{-6} $\text{nm}_{\text{rms}}\,\text{Hz}^{-1/2}$) and the photodiode shot noise (2×10^{-6} $\text{nm}_{\text{rms}}\,\text{Hz}^{-1/2}$). The increase in the noise below 700 Hz is presumably due to the position fluctuations of the laser spots on the photodiodes. However, since the vibrations of the free cantilever are at least 1 order of magnitude greater, we do not investigate the origin of this noise in more detail.

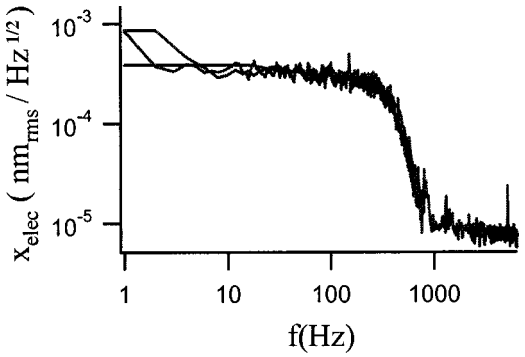

FIG. 3. The equivalent displacement noise spectrum when the two beams are sent on the same mirror. It represents the noise of the interferometer without cantilever motion.

C. Displacement sensor

The relative separation between the extremities of the two cantilevers C_1 and C_2 is measured with an original capacitive sensor. The capacitance is formed by the duralumin plates which are fixed on the two cantilevers, so that when surfaces are brought together, the displacement of the surfaces is equal to the displacement of the capacitor's plates. The distance d between the two plates is typically $d = 100$ μm. Such a large distance avoids capillary condensation between the plates. A system of canals and holes tooled in the moving plate minimizes the hydrodynamic drag between the capacitor plates. This capacitor is included in a Clapp oscillator. The frequency f of the oscillations is

$$f = \frac{1}{2\pi\sqrt{L(1/C_a + 1/C_b + 1/C)^{-1}}}, \quad (2)$$

where $L = 2.2$ μH is a fixed inductance, $C_a = C_b = 220$ pF two fixed capacitances, and $C = 2.5 \times 10^{-14}/d$, with C expressed in Farad. For a typical value of $d = 100$ μm the oscillator's frequency is $f = 12$ MHz and the sensitivity is constant $\Delta f/\Delta d \approx 20$ Hz/nm. The frequency is first measured with a HP53132A counter, which reads frequency variations of $\Delta f = 1$ Hz (corresponding to a variation of the distance between capacitor plates $\Delta d = 0.05$ nm) on a 0.1 s acquisition time. This reading allows us to measure the mean distance between surfaces, but cannot be used for a determination of dynamical properties on time scales smaller than the time of acquisition of 0.1 s. For this reason, the oscillator frequency is also measured with a fast frequency to voltage converter. To make this frequency to voltage conversion, the frequency of the oscillator is first shifted around 10 kHz, and then converted to voltage with a digital phase lock loop. The

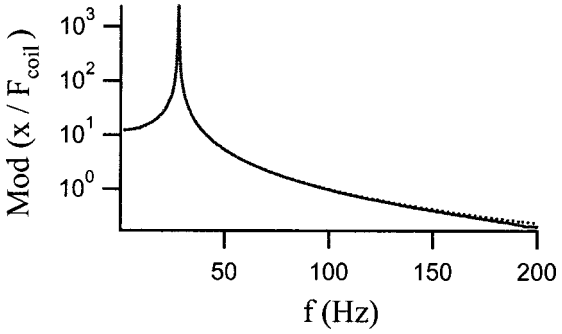

FIG. 4. Frequency response of the cantilever: (straight line) the measurement, and (dashed line) the best fit of the mass-spring-damping model.

overall sensitivity of this sensor is $\Delta V/\Delta f \approx 5$ mV/nm. Indeed, the sensitivity of this sensor depends on the distance between capacitor plates. This sensitivity is calibrated by imposing a displacement to the force cantilever C_2, which is read simultaneously with the capacitive and the optical sensor. Since the optical sensor measures the absolute displacement, the sensitivity of the capacitive sensor is determined. More details about the electronics of the oscillator and the frequency voltage converter may be found elsewhere.[8]

D. Cantilever

The force cantilever requirement is to have a high resonant frequency. This is necessary for small time scale dynamic studies. This can be achieved by a high stiffness of the cantilever. The drawback of a high stiffness is that it diminishes the resolution of the force measurement. We choose a compromise with a stiffness of $K=2000$ N/m. The cantilevers are composed of two bending spring which are BeCu foils of 0.6 mm thickness. The measurements of the mechanical characteristics of the force cantilever are performed with the surfaces and the capacity plates far away. A driving force $F_{\text{coil}}=F_0 e^{j\omega t}$ is applied with the coil–magnet system, and the force cantilever displacement is measured. The amplitude response of the free cantilever as a function of frequency is shown as the plain line in Fig. 4. A resonance is seen at $f_{\text{res}}=28$ Hz with a flat response below. A simple mass-spring-damping model matches the mechanical behavior of the cantilever up to 200 Hz. However, at higher frequencies, other vibration modes take place.

The stiffness K and mass M are determined with the measurement of frequency resonance f_{res} when small calibrated weights m are added onto the cantilever extremity. A linear fit of m as a function of f_{res}^{-2} allows us to determinate both the stiffness $K=1940\pm 30$ N/m and the equivalent mass $M=61\pm 2$ g. These quantities evolve sufficiently slowly with time in order that this calibration procedure is only needed a few times a year.

III. MEASUREMENTS AND LIMITATIONS

The cantilever displacement x is related to the force $F_s(h)$ acting between surfaces according to the dynamic equation

$$M\ddot{x} = -\lambda\dot{x} - Kx + F_s(h) + \delta f, \tag{3}$$

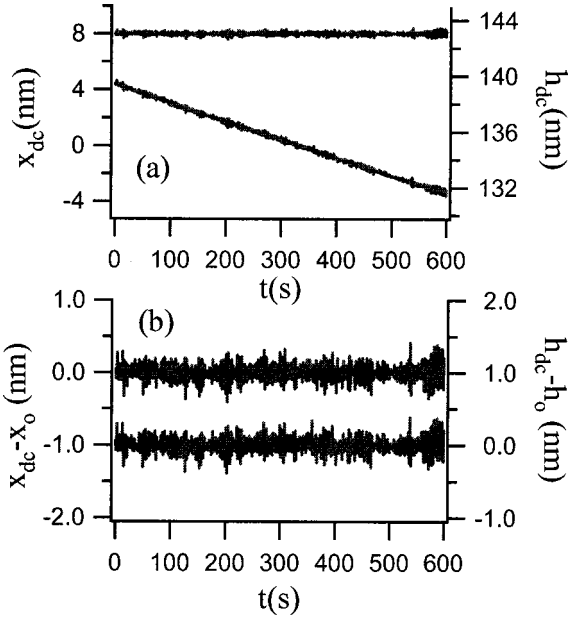

FIG. 5. Typical drift and noise signals of the two sensors outputs.

where $\dot{x}$ is the time derivate of x, M, λ, and K are issued from the mechanical model for the mass-damping-spring system, and δf designs the sum of other extra forces acting on the cantilever. The sensible contributions to δf are, in the first part, the inertial force induced by the vibrations of the DSFA frame, and in the second part interactions between the capacitor plates. During a typical experiment, the piezoelectric crystals are driven in such a way that the displacement is twofold: a slow approach or recession of surfaces (in the following referred to as static displacement), and a small harmonic displacement (dynamic displacement). These two components of the displacement, and the two associated components of the force, are collected simultaneously during an experiment. In the following section we discuss the way to acquire sensor outputs and the influence of thermal drift and extra forces on the overall resolution of the apparatus.

A. Static measurements

The static components of the surface force F_s and of the relative displacement of surfaces h are obtained from the averaged values x_{dc} and h_{dc} of optic and capacitive sensors. For this, the outputs of the sensors are synchronously collected with a 16 bit acquisition card,[11] and averaged on a 1 s acquisition time. Figure 5 shows a typical temporal evolution of signals when no relative motion is imposed on the surfaces. The displacement x of the cantilever and the separation h between the surfaces are related to the outputs of the sensors accordingly to $x=x_{\text{dc}}-x_0$ and $h=h_{\text{dc}}-h_0$, where x_0 and h_0 are two unknown shifts. The drift rates of these shifts are measured at the beginning and at the end of an experiment and the signals are corrected from it. With a simple plexiglas cover, drift rates are constant for 1 h, with typical values of 0.01 nm/s. This is of the same order of magnitude as the best values reported for interferometric SFA by Heuberger *et al.*[12]

The remaining noises on x and h are not due to sensors but correspond to vibrations of the cantilever spring. Indeed,

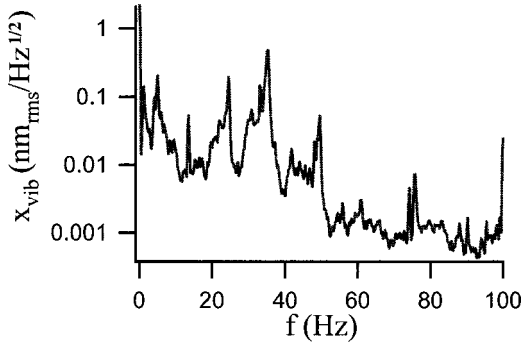

FIG. 6. Mechanical noise spectrum of the free force cantilever.

noises on x and h are perfectly correlated, and are at least 1 order of magnitude greater than the intrinsic noise of sensors. Their magnitudes $x_{\mathrm{rms}}=h_{\mathrm{rms}}=0.12$ nm are large compared to expected thermal noise $(kT/K)^{1/2}\approx 4$ pm, and this noise is due to soil vibrations not filtered by our antivibration stage. It must be stressed, that, since vibrations act as inertial forces on the free cantilever C_2, increasing the cantilever stiffness may improve the resolutions of the distances measurements, but not the resolution of the force measurement.

B. Dynamic measurements

The dynamic measurements are obtained from two double lock-in amplifiers synchronized on the piezoelectric harmonic excitation. We introduce complex notations for the alternative components of h and x:

$$h_{\mathrm{ac}}(t)=\hat{h}e^{j\omega t},$$
$$x_{\mathrm{ac}}(t)=\hat{x}e^{j\omega t}, \tag{4}$$

where $\hat{h}$ and $\hat{x}$ are complex variables giving both amplitude and relative phases of the variables. Substituting Eq. (4) into Eq. (3) results in

$$\frac{\hat{F}_s}{\hat{h}}=\frac{\hat{x}}{\hat{h}}(K+j\omega\lambda-M\omega^2)-\frac{\hat{\delta f}}{\hat{h}}, \tag{5}$$

where $\hat{F}_s/\hat{h}$ is the transfer function of the surface force interactions and $\hat{\delta f}$ the alternative component of δf.

The significant contributions of δf, which needs to be taken into account for a determination of the function transfer $\hat{F}_s/\hat{h}$, are twofold. First, interactions between capacity plates take place: the air flow between the capacity plates induces a hydrodynamic viscous force $\delta f_{\mathrm{capa}}=-\Lambda\dot{h}$. This one is measured in the absence of surfaces and its constant contribution $-j\omega\Lambda$ is subtracted from the transfer function. Second, vibrations act as a force δf_{vibr}. This contribution may be evaluated by the measurement of the cantilever vibration x_{vibr} in the absence of surfaces. Figure 6 shows the power density spectrum of x_{vibr} as a function of the frequency. Resonance peaks are visible, and the corresponding frequencies are avoided for dynamical studies. Typically, the corresponding force resolution is 10 nN for a 1 Hz bandwidth.

IV. A FORCE MEASUREMENT TEST

We present, as a test of the above experimental setup, a study of the hydrodynamics of a liquid film confined between solid surfaces. Surfaces are a plane and a sphere (radius $R=1.35$ mm) of Pyrex glass. First, surfaces are washed for a few hours in an ultrasonic bath with a detergent soap, and then carefully rinsed with propanol. Finally they are passed through a flame in order to flatten the surfaces. A measurement of the roughness performed with an atomic force microscope shows a typical 0.3 nm roughness on a 1 $\mu\mathrm{m}^2$ square. Surfaces are quickly mounted on the surface holders and a small drop of *n*-dodecane is introduced between the surfaces. This drop is small enough to stick to the surfaces The thermal equilibration with the room temperature ($T=25.0\,^{\circ}\mathrm{C}$) occurs after few hours of an important thermal drift. The experiments begin with surfaces separated by a distance of 500 nm. Surfaces are then approached at a constant velocity $\dot{h}_{\mathrm{dc}}=0.2$ nm/s. During the same time we add a small harmonic oscillation with an amplitude $|\hat{h}|=0.8$ nm and at a frequency $f=\omega/(2\pi)=64$ Hz.

Previous studies have shown that for surface separations $h>5.0$ nm, the liquid is purely Newtonian and the flow of liquid may be described within the lubrication approximation.[3,13] In this framework, the hydrodynamic force F_{hyd} between the surfaces may be expressed as[13]

$$F_{\mathrm{hyd}}=-\frac{6\pi\eta R^2}{h}\frac{dh}{dt}, \tag{6}$$

where η is the bulk viscosity of the liquid and R the sphere radius. Noting that $\dot{h}\approx\dot{h}_{\mathrm{ac}}$, the resulting complex transfer function may be expressed as

$$\hat{F}_{\mathrm{hyd}}/\hat{h}=-j6\pi\eta R^2/h. \tag{7}$$

The complex amplitudes $\hat{x}$ and $\hat{h}$ are measured and the transfer function $\hat{F}/\hat{h}$ of the surfaces forces is computed from Eq. (5). First, we observed that the measured force is out of phase with the displacement. This means that the measured force is purely dissipative and that nonhydrodynamic forces are negligible in our experiment. Figure 7 is a plot of the inverse of the imaginary part of $\hat{F}/\hat{h}$ as a function of the surface separation during the approach and recession of surfaces. As expected from the lubrication theory [Eq. (6)], the plot is a straight line. The slope of the linear fit of experimental data allows a determination of the liquid viscosity $\eta=1.37\times10^{-3}$ Pa s in accordance with the tabulated one $\eta=1.37\times10^{-3}$ Pa s at ($T=25.0\,^{\circ}\mathrm{C}$). The extrapolation of this linear behavior at infinite dissipation determines the contact point $h=0$ between the two hydrodynamic walls. As seen in the inset of Fig. 7, the linear model described by Eq. (7) holds for separations $h>7.0$ nm. Deviations to Eq. (7) occurs at a smaller distance where both the application of macroscopic hydrodynamic and the linearization of Eq. (7) are expected to fail. We do not discuss the problem of the location of the hydrodynamic boundaries compared to the solid surfaces. This question may be addressed if we know the origin of the displacement between surfaces, information

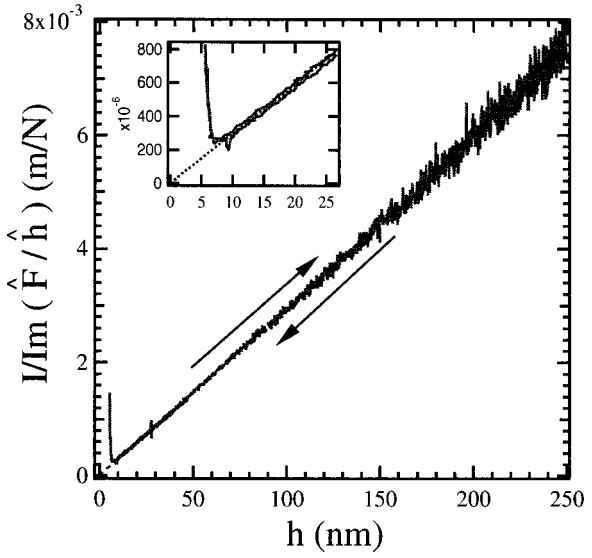

FIG. 7. Plot of the inverse of the imaginary part of $\hat{F}/\hat{h}$ as a function of the surfaces separation h when the surfaces are approached and receed. (Inset) A zoom of the zone near the origin. The dashed line represents the best linear fit of the data.

which may be obtained from the measurement and the modelization of the static force during the contact between the surfaces.

V. DISCUSSION

A SFA allowing dynamical studies of confined media has been described. Two different sensors with high resolutions give simultaneous access, after a simple treatment, to both the separation and the force between the surfaces. The large frequency ranges of these sensors permit us to measure the response to rapid deformation. As a test example, we use this apparatus as a variable gap rheometer, and investigate a simple Newtownian fluid. This simple application suggests that this apparatus is a powerful tool for studying complex fluids under confinement.

ACKNOWLEDGMENTS

The authors thank J. L. Loubet and A. Tonck for helpful discussions, the workshops of ENSL and DPM for mechanical and electronic design, and S. Jurine for help with the experiments. This project has been supported by MENRT (program DUAL).

[1] J. N. Israelachvili and D. Tabor, Proc. R. Soc. London, Ser. A **331**, 19 (1972).
[2] D. Tabor and R. H. S. Winterton, Proc. R. Soc. London, Ser. A **312**, 435 (1969).
[3] A. Tonck, J. M. Georges, and J. L. Loubet, J. Colloid Interface Sci. **126**, 1 (1988).
[4] A. M. Stewart, Meas. Sci. Technol. **11**, 298 (2000).
[5] P. Frantz, N. Agrait, and M. Salmeron, Langmuir **12**, 3289 (1996).
[6] P. Frantz, A. Artsyukhovich, R. W. Carpick, and M. Salmeron, Langmuir **13**, 5957 (1997).
[7] G. Nomarski, J. Phys. Radium **16**, 95 (1955).
[8] F. Restagno, J. Crassous, E. Charlaix, and M. Monchanin, Meas. Sci. Technol. **12**, 16 (2001).
[9] C. Schöenberger and S. F. Alvarado, Rev. Sci. Instrum. **60**, 3134 (1989).
[10] S. P. Jarvis, A. Oral, T. P. Weihs, and J. B. Pethica, Rev. Sci. Instrum. **64**, 3515 (1993).
[11] Micromotor: Newfocus MRA actuator 8321; Piezoelectric: Physik Instrumente P24910; Laser: Melles Griot 05STP901; Photodiodes: Hamamatsu S112-44BK; Voltage divisor: Analog Device AD534; Acquisition card: HPe1415A.
[12] M. Heuberger, M. Zäch, and N. D. Spencer, Rev. Sci. Instrum. **71**, 4502 (2000).
[13] D. Y. C. Chan and R. G. Horn, J. Chem. Phys. **83**, 5311 (1985).